Available online at www.sciencedirect.com

ScienceDirect

Mendeleev Commun., 2023, **33**, 255–258

Mendeleev Communications

Doxorubicin compositions with biocompatible terpolymer of *N*-vinylpyrrolidone, methacrylic acid and triethylene glycol dimethacrylate

Svetlana V. Kurmaz,*[a] Irina I. Ivanova,[a] Nina S. Emelyanova,[a] Dmitry V. Konev,[a] Vladimir A. Kurmaz,[a] Natalia V. Filatova,[a] Anastasia A. Balakina[a] and Alexei A. Terentiev[a,b,c]

[a] *Federal Research Center of Problems of Chemical Physics and Medicinal Chemistry, Russian Academy of Sciences, 142432 Chernogolovka, Moscow Region, Russian Federation. Fax: +7 496 522 3507; e-mail: skurmaz@icp.ac.ru*

[b] *Department of Fundamental Physical and Chemical Engineering, M. V. Lomonosov Moscow State University, 119991 Moscow, Russian Federation*

[c] *Scientific and Educational Center, Moscow State Regional University, 141014 Mytishchi, Moscow Region, Russian Federation*

DOI: 10.1016/j.mencom.2023.02.034

Compositions of doxorubicin with a terpolymer of *N*-vinylpyrrolidone, methacrylic acid and triethylene glycol dimethacrylate have been prepared and investigated by UV-VIS and NMR spectroscopy, cyclic voltammetry and DFT quantum chemical modeling. Oxygen containing groups of the terpolymer and hydrogen atoms of the drug OH and NH_3^+ groups form hydrogen bonds. The compositions have lower cytotoxicity *in vitro* compared with that of free doxorubicin.

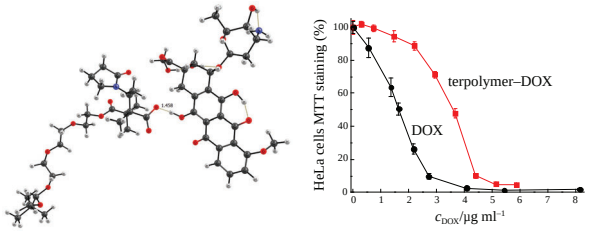

Keywords: *N*-vinylpyrrolidone, triethylene glycol dimethacrylate, terpolymer, doxorubicin, quantum chemical modeling, cyclic voltammetry, cytotoxicity.

Doxorubicin (DOX) is an anthracycline antibiotic with antitumor and antileukemic activity.[1] It has adverse effects such as cardiotoxicity, hypoallergic reactions and general disturbance of wellbeing. To diminish its general toxicity as well as increase the selectivity and circulation time in a bloodstream, DOX is typically introduced into various nanocarriers such as liposomes,[2,3] phospholipid nanoparticles,[4] dendrimers,[5–7] microgels,[8] hydrogels,[9] polyelectrolyte multilayer capsules of dextran sulfate and poly-L-arginine,[10] boron nitride nanoparticles,[11] graphene and graphene oxide[12] as well as silver and gold nanoparticles,[13] details being given in reviews.[14,15]

As the antitumor drug carriers, biocompatible nanocontainers based on synthetic and natural polymers have been designed.[16,17] In this work, we propose a terpolymer of *N*-vinylpyrrolidone (VP), methacrylic acid (MAA) and triethylene glycol dimethacrylate (TEGDM) as a DOX carrier. We found that branched VP copolymers of different composition, molecular weight and topology were biocompatible and affected insignificantly the viability of normal Vero cells as well as the A172 or HeLa tumor ones.[18–23] Organic complexes of platinum(IV) encapsulated in these copolymers have less cytotoxicity compared with the free compounds.[19–21] 3D structure of macromolecules and the size of their aggregates in aqueous media correspond to the main criteria for delivery vehicles and are related to the clearance in kidneys and spleen,[24–26] while small polymer particles can circulate in a bloodstream for the time sufficient to ensure the effect of their encapsulated drugs.[27]

The 3D terpolymer was obtained here using the known technique[22] by radical copolymerization of the three monomers

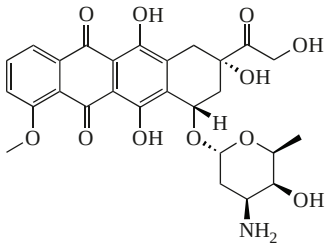

DOX

in ethanol at a molar ratio VP : MAA : TEGDM of 98 : 2 : 2 (for details of the synthesis and isolation, see Online Supplementary Materials). The copolymer had 3.8 wt% MAA units according to potentiometric titration, molar ratio of VP to (di)methacrylate units of 85.6 : 14.4, M_w of 76.0 kDa, critical aggregation concentration (CAC) in water of 5.0 mg ml^{-1} and hydrodymamic radius R_h of 10 nm as measured in aqueous neutral PBS at 5.0 mg ml^{-1}.

Commercial DOX hydrochloride (Teva Parmaceuticals) used in this work contained lactose monohydrate (~360 Da). According to IR spectroscopy, hydrogen bonds can be assumed between the OH groups of lactose and C=O groups of VP units in the solid polymer compositions. Despite this, the interaction with water should be stronger than with the amphiphilic copolymer and free lactose does not affect the formation of the drug polymer composition.

Two series of the compositions were prepared, namely, PC1DOX$_n$ with n = 0.6, 1.3, 1.9, 2.5 and 3.1 wt% DOX originated from 2 mg ml^{-1} solutions of the copolymer in Pr^{i}OH as well as PC2DOX$_n$ with n = 0.5, 1.25, 2.5 and 5.0 wt% DOX on the basis

of terpolymer solutions of various concentrations (for details, see Tables S1 and S2, Online Supplementary Materials). Solutions with no copolymer containing the corresponding amounts of DOX were used as a control.

Aqueous buffer solutions of $PC1DOX_n$ and $PC2DOX_n$ were analyzed by UV-VIS spectroscopy using the DOX absorption band maximum at ~490 nm [Figures 1 and S2(*a*)]. As follows from Figure 1, with an increase in DOX content for $PC1DOX_n$, optical density *A* of its absorption band grows. Besides, the *A* value is higher for the solutions of $PC1DOX_{2.5}$ and $PC1DOX_{3.1}$ compared with that for the same amounts of free DOX in the control experiments (see Figure 1, dashed lines corresponding in their colors to $PC1DOX_{2.5}$ and $PC1DOX_{3.1}$). This difference originates from DOX inclusion in the copolymer structure and influence of the polymer environment on molar extinction coefficient of the DOX chromophore. The function of *A vs.* DOX concentration in solution is linear in the control experiments (Figure S1), while the molar extinction coefficient increases as a result of a decrease in the polarity of polymer matrix. In the second series of solutions, namely with $PC2DOX_n$, the *A* value of the DOX absorption band is higher than that for free DOX [see Figure S2(*a*)] and the dependence of *A vs*. the copolymer concentration is complex [Figure S2(*b*)]. These data indicate the drug association with the terpolymer through physical entrapment within the polymer matrix and penetration of the DOX molecules into cavities with formation of guest–host type complexes as well as the drug adsorption on the surface of nanoparticles. Pr^iOH as a poor solvent for DOX can promote its association with the terpolymer. Besides, the macromolecules are more compact in such a solvent, which makes it possible to diminish the size of the 3D cavities and stimulates intermolecular interactions in the system.

To determine effective binding constant K_{eff}, the dependence $1/(A - A_0)$ *vs.* 1/[DOX] was plotted, where *A* and A_0 represented the optical densities at 490 nm for DOX and the copolymer, respectively. In correspondence with calculation details and expression from the review book,[28] the ratio of the intercept to the slope gave the K_{eff} value of 5.6×10^3 dm^3 mol^{-1} at 22 °C.

According to dynamic light scattering (DLS) data (Figure S3), the scattering intensity of $PC1DOX_{3.1}$ solution is poorly dependent on temperature, while the scattering centers size reaches 70 nm under ambient conditions. ^{1}H NMR data of $PC1DOX_{3.1}$ in $CDCl_3$ (Figure S4, spectrum *2*) reveals signals related to DOX and the VP units[19] of the terpolymer.

Figure 2 shows cyclic voltammogram (CVA) curves for DOX and $PC1DOX_{3.1}$ in PBS on a glassy carbon electrode at scan rate $v = 100$ mV s^{-1}. The respective data at scan rates of 10–2000 mV s^{-1} are collected in Figure S5. CVA curves for PBS, PBS + terpolymer or PBS + terpolymer + lactose as background electrolytes [see Figure S5(*c*)] do not contain any redox peaks within all the potential range from *ca*. –1 to +1 V. Two peak couples are observed in the positive [see Figure S5(*a*),(*b*), peaks pa2 and pc2] as well as negative [see Figure S5(*a*),(*b*), peaks pc1 and pa1] areas of the redox potentials associated with oxidation of hydroquinone centers and reduction of quinone moiety in the DOX molecule.[29,30] They contain nearly reversible reduction–oxidation peaks at *ca*. –0.6 V and nearly irreversible ones for oxidation–reduction in the range of *ca*. +0.3 to +0.6 V. In the complex, the DOX guest is more difficult to oxidize and its reduction is facilitated [see Figure 5S(*b*), peaks pc1 and pa1], which leads to a greater reversibility of the process compared with the free drug. In the anode region, the oxidation of hydroquinone center is facilitated and the reduction of DOX is complicated [see Figure S5(*a*), peaks pa2 and pc2]. This may be due to participation of the groups in formation of a hydrogen bond as well as its stretching and weakening. Moreover, the nature of the electrode process changes from the adsorption for free DOX to the diffusion–adsorption for the complex $PC1DOX_{3.1}$ as it follows from slopes of the lg*I* *vs*. lg*v* dependences equal to 0.92 and 0.74, respectively.

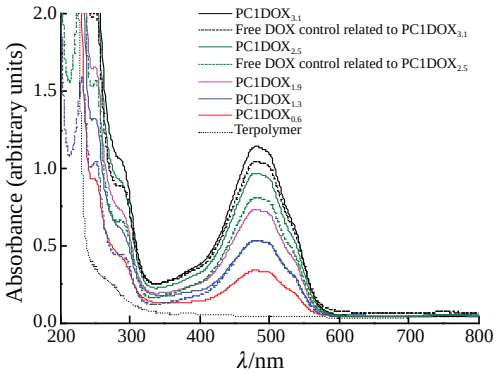

Figure 1 UV-VIS spectra of aq. PBS solutions of the terpolymer, free DOX as well as $PC1DOX_n$ with $n = 0.6$, 1.3, 1.9, 2.5 and 3.1 wt% DOX. The spectra of free DOX solutions in control experiments (see Table S1) are shown by the corresponding dashed lines.

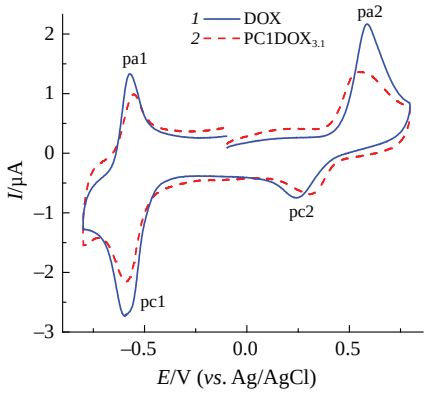

Figure 2 CVA curves at 100 mV s^{-1} for aq. PBS solutions of (*1*) 4.0×10^{-5} mol dm^{-3} DOX and (*2*) $PC1DOX_{3.1}$ with DOX concentration of 1.4×10^{-5} mol dm^{-3}.

The results of quantum chemical (QTAIM) modeling of $PCDOX_n$ reveal that the formation of hydrogen bonds of various strength and energy between oxygen containing groups of the terpolymer as electron donors and hydrogen atoms of OH and NH_3^+ groups of DOX are possible (for details, see Online Supplementary Materials). Table 1 shows the values of the energies for the hydrogen bonds. MAA units represent the main donor of electronic density (Figure S6), which generates the most strong and numerous bonds with the drug compared to carbonyl group of the lactame ring of VP units. Intermolecular structures are also formed between TEGDM units and DOX, however, the energy of these hydrogen bonds is lower. The counterpart interactions between oxygen atoms of DOX and hydrogen atoms of the terpolymer, according to calculations, are still weaker and do not exceed 3 kcal mol^{-1}. Meanwhile, the

Table 1 Energy of the hydrogen bonds formed between oxygen atoms of the copolymer and hydrogen atoms of DOX.

Terpolymer units	Terpolymer groups as electron donors	DOX groups as electron acceptors	E_{bond} (QTAIM)/ kcal mol^{-1}
MAA	COOH	CH, OCH_3, OH^-, NH_3^+	8.8, 13.3, 12.3, 25.5, 22.1
VP	C=O	OH, OCH_3, NH_3^+	11.8, 9.4, 6.9
TEGDM	C–O–C	OH^-	1.2, 1.3, 3.5, 6.2

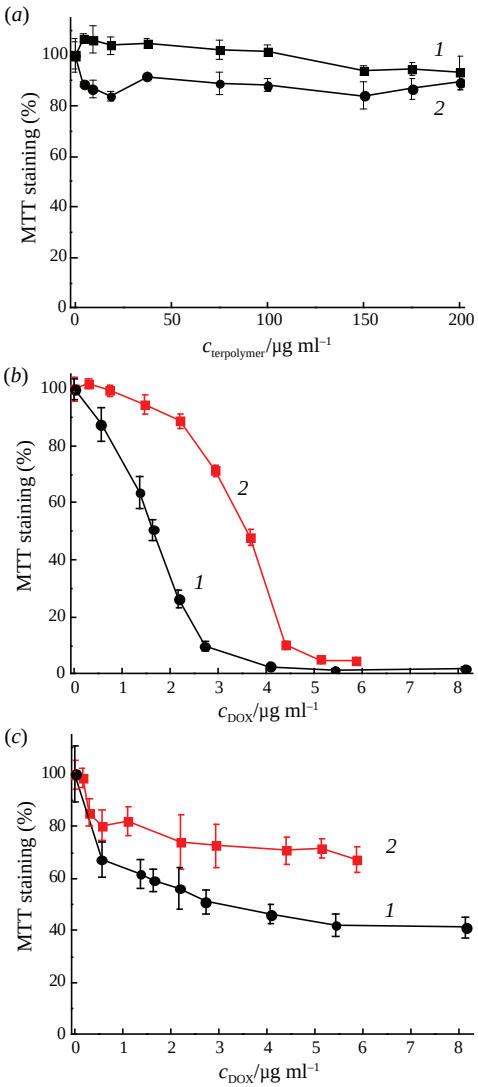

Figure 3 MTT staining after 24 h action of (*a*) the terpolymer on (*1*) HeLa and (*2*) Vero cells, (*b*) (*1*) DOX and (*2*) PC1DOX$_{3.1}$ on HeLa cells as well as (*c*) (*1*) DOX and (*2*) PC1DOX$_{3.1}$ on Vero cells.

known maximum values of E_{bond} for DOX in the VP–TEGDM copolymer complex[31] do not exceed 12 kcal mol^{-1}.

Cytotoxic effect of the terpolymer, free DOX and PC1DOX$_{3.1}$ was investigated using tumor HeLa cells and the noncancerous Vero ones *in vitro*. The dose–response curves are given in Figure 3 and IC$_{50}$ values are collected in Table S3. The terpolymer has no cytotoxic effect on both tumor and normal cells [see Figure 3(*a*)] in the entire range of concentrations explored and thus does not contribute significantly to the cytotoxicity of PC1DOX$_{3.1}$, similar to other biocompatible and/or biodegradable polymers like polylactide.[32] Free DOX has higher toxicity to HeLa tumor cells compared with the Vero ones. PC1DOX$_{3.1}$ is less cytotoxic than free DOX for both cell lines [Figure 3(*b*),(*c*)]. For HeLa cells, both free DOX and PC1DOX$_{3.1}$ have the dose–response curves with a classic S-shape, while for the Vero ones under the action of both compounds the curves flatten out. With PC1DOX$_{3.1}$ and Vero cells, it was not possible to achieve 50% decrease in the cell viability within 24 h. The differences in the effects of free DOX and PC1DOX$_{3.1}$ seem to be related to the delayed drug release from the polymer carrier due to necessity of the DOX–terpolymer hydrogen bonds destruction and the drug diffusion from the carrier.

In summary, the compositions of DOX with an amphiphilic copolymer VP–MAA–TEGDM have been designed and characterized. Experimental data and quantum chemical calculations indicate the formation of complexes, in which oxygen containing groups of the terpolymer monomer units and hydrogen atoms of the DOX OH and NH_3^+ groups form hydrogen bonds. The strongest bonds arise for the carboxyl group of MAA. The polymer–DOX composition reveals less cytotoxicity *in vitro* compared with the free drug. The resulting systems may be used for investigation of their toxicity *in vivo* as well as development of modern approaches to control the selectivity of their action and reduce the general toxicity of the anticancer drug.

This work was carried out within the framework of topics AAAA-A19-119041090087-4, AAAA-A19-119071890015-6 and AAAA-A19-119061890019-5 of the State Assignment.

Online Supplementary Materials

Supplementary data associated with this article can be found in the online version at doi: 10.1016/j.mencom.2023.02.034.

References

1 S. K. Carter and R. H. Blum, *Ca-Cancer J. Clin.*, 1974, **24**, 322.
2 P. G. Tardi, N. L. Boman and P. R. Cullis, *J. Drug Targeting*, 1996, **4**, 129.
3 Y. Barenholz, *J. Controlled Release*, 2012, **160**, 117.
4 N. V. Medvedeva, T. I. Torkhovskaya, L. V. Kostryukova, T. S. Zakharova, V. A. Kudinov, E. O. Kasatkina, V. N. Prozorovskiy and O. M. Ipatova, *Biomed. Khim.*, 2017, **63**, 56 (in Russian).
5 N. G. Yabbarov, E. D. Nikolskaya, O. A. Zhunina, I. G. Kondrasheva, I. A. Zamulaeva and E. S. Severin, *Russ. J. Bioorg. Chem.*, 2017, **43**, 155 (*Bioorg. Khim.*, 2017, **43**, 180).
6 N. G. Yabbarov, G. A. Posypanova, E. A. Vorontsov, O. N. Popova and E. S. Severin, *Biochemistry*, 2013, **78**, 884 (*Biokhimiya*, 2013, **78**, 1128).
7 P. Tambe, P. Kumar, K. M. Paknikar and V. Gajbhiye, *J. Controlled Release*, 2019, **299**, 64.
8 Z.-Y. Qiao, R. Zhang, F.-S. Du, D.-H. Liang and Z.-C. Li, *J. Controlled Release*, 2011, **152**, 57.
9 M. Si, Y. Xia, M. Cong, D. Wang, Y. Hou and H. Ma, *Int. J. Nanomed.*, 2022, **17**, 1309.
10 D. B. Trushina, R. A. Akasov, A. V. Khovankina, T. N. Borodina, T. V. Bukreeva and E. A. Markvicheva, *J. Mol. Liq.*, 2019, **284**, 215.
11 I. Yu. Zhitnyak, I. V. Sukhorukova, A. M. Koval'skiy, A. T. Matveev, I. N. Bychkov, D. V. Shtanskiy and N. A. Glushankova, *Usp. Mol. Onkol.*, 2016, **3** (2), 34 (in Russian).
12 J. Liu, L. Cui and D. Losic, *Acta Biomater.*, 2013, **9**, 9243.
13 U. Kanwal, N. I. Bukhari, M. Ovais, N. Abass, K. Hussain and A. Raza, *J. Drug Targeting*, 2018, **26**, 296.
14 K. Chen, H. Cai, H. Zhang, H. Zhu, Z. Gu, Q. Gong and K. Luo, *Acta Biomater.*, 2019, **84**, 339.
15 C. Carvalho, R. X. Santos, S. Cardoso, S. Correia, P. J. Oliveira, M. S. Santos and P. I. Moreira, *Curr. Med. Chem.*, 2009, **16**, 3267.
16 A. S. Popov, A. A. Efimova, A. V. Kazantsev, D. A. Erzunov, N. V. Lukashev, I. D. Grozdova, N. S. Melik-Nubarov and A. A. Yaroslavov, *Mendeleev Commun.*, 2021, **31**, 827.
17 V. V. Spiridonov, K. S. Sadovnikov, D. A. Vasilenko, K. N. Sedenkova, A. R. Lukmanova, A. A. Markova, A. V. Shibaeva, A. V. Bolshakova, S. S. Karlov, E. B. Averina and A. A. Yaroslavov, *Mendeleev Commun.*, 2022, **32**, 591.
18 S. V. Kurmaz, N. A. Obraztsova, A. A. Balakina and A. A. Terent'ev, *Russ. Chem. Bull.*, 2016, **65**, 2097.
19 S. V. Kurmaz, N. V. Fadeeva, B. S. Fedorov, G. I. Kozub, N. S. Emel'yanova, V. A. Kurmaz, R. A. Manzhos, A. A. Balakina and A. A. Terentyev, *Mendeleev Commun.*, 2020, **30**, 22.
20 S. V. Kurmaz, V. D. Sen', A. V. Kulikov, D. V. Konev, V. A. Kurmaz, A. A. Balakina and A. A. Terent'ev, *Russ. Chem. Bull.*, 2019, **68**, 1769.
21 S. V. Kurmaz, D. V. Konev, V. A. Kurmaz, G. I. Kozub, V. M. Ignat'ev, N. S. Emel'yanova, A. A. Balakina and A. A. Terentyev, *INEOS Open*, 2021, **4**, 195.
22 S. V. Kurmaz, I. I. Ivanova, N. V. Fadeeva, E. O. Perepelitsina, M. A. Lapshina, A. A. Balakina and A. A. Terent'ev, *Polym. Sci., Ser. A*, 2022, **64**, 434 (*Vysokomol. Soedin., Ser. A*, 2022, **64**, 333).
23 S. V. Kurmaz, N. V. Fadeeva, A. V. Komendant, V. M. Ignatiev, N. S. Emelyanova, G. V. Shilov, T. S. Stupina, N. V. Filatova, M. A. Lapshina and A. A. Terentyev, *Polym. Bull.*, 2022, **79**, 8905.
24 N'D. S. Irvin-Choy, K. M. Nelson, J. P. Gleghorn and E. S. Day, *J. Mater. Chem. B*, 2020, **8**, 6548.

25 E. Blanco, H. Shen and M. Ferrari, *Nat. Biotechnol.*, 2015, **33**, 941.
26 N. Hoshyar, S. Gray, H. Han and G. Bao, *Nanomedicine*, 2016, **11**, 673.
27 S. V. Kurmaz, N. V. Fadeeva, Ju. A. Skripets, R. I. Komendant, V. M. Ignatiev, N. S. Emel'yanova, Yu. V. Soldatova, I. I. Faingold, D. A. Poletaeva and R. A. Kotelnikova, *Mendeleev Commun*., 2022, **32**, 117.
28 K. A. Connors, *Binding Constants: The Measurement of Molecular Complex Stability*, John Wiley & Sons, 1987.
29 G. M. Rao, J. W. Lown and J. A. Plambeck, *J. Electrochem. Soc*., 1978, **125**, 534.
30 A. M. Oliveira-Brett, J. A. P. Piedade and A.-M. Chiorcea, *J. Electroanal. Chem*., 2002, **538**–**539**, 267.
31 V. M. Ignat'ev, N. S. Emel'yanova, S. V. Kurmaz and N. V. Fadeeva, *Russ. Chem. Bull*., 2021, **70**, 1269.
32 A. A. Chernyshev, D. N. Lytkina, A. S. Buiakov, S. N. Kulkov and I. A. Kurzina, *Mendeleev Commun*., 2021, **31**, 881.

Received: 13th October 2022; Com. 22/7024